

Estimation of Mechanical Properties of Microplasma Welding of 0.5 mm SS304 Sheets

Kasif Ansari¹ , Mayuri Baruah¹ 

¹ National Institute of Technology, Production and Industrial Engineering Department, Jamshedpur, Jharkhand, India.

How to cite: Ansari K, Baruah M. Estimation of mechanical properties of microplasma welding of 0.5 mm SS304 sheets. *Soldagem & Inspeção*. 2023;28:e2803. <https://doi.org/10.1590/0104-9224/SI28.03>

Abstract: The demand for light weight and small components has increased tremendously over the years. The present work describes the plasma micro welding of SS304 alloy. Plasma arc micro welding is carried out on thin sheet to characterize the effect of welding parameters. The proper ranges of welding current at constant welding speed for two different plasma gas flow rates are evaluated to obtain better quality of weld at butt joint configuration. Distortion is a major problem for welded structures especially for the thinner materials. Hence, the variation of process parameters viz. welding current and plasma gas flow rate are studied on weld-induced distortion. Distortion analysis both longitudinal shrinkage and transverse shrinkage are done for six different welding conditions. It is predicted that both longitudinal shrinkage and transverse shrinkage increases with increase in plasma gas flow rate and current. The tensile strength and microstructure are also determined at different gas flow rates and welding currents. This may be due to the application of more heat at higher values.

Keywords: Micro welding; Distortion; Longitudinal shrinkage; Transverse shrinkage; Residual stress.

1. Introduction

Welding is one of the oldest processes adapted by humans as an obscure art or a crude construction technique. Bending and distortions are inevitable in welding due to the large temperature variation within a small zone. Researchers from all over the world are eyeing the field of welding-induced residual stress and deformation. For the better understanding of the underlying physics associated with welding distortion, various numerical and experimental studies have been carried out. An artificial neural network method is utilized to investigate the distortion of welded SS304 thin sheets [1]. Murugan and Gunaraj [2] conducted experiment as per the design matrix controlled GMAW equipment and they identified the process parameters. They found the highest and lowest values and accordingly did the experiment to record the response viz. angular distortion. Deng [3] observed that in case of low carbon steel transformation temperature range is quite vast compared to other carbon steel and because of martensitic transformation, dilution is low and so the phase transformation does not have a significant effect on the distortion. Long et al. [4] highlighted the transverse, longitudinal and angular distortions induced in thick butt welded low carbon steel plates by performing a three dimensional finite element analysis. Using thermo elastic-plastic large deformation techniques, three dimensional finite element simulations had been performed by Deng and Murakawa [5] They calculated the angular distortions (1 mm thick butt low carbon steel plate) due to the introduction of welding. In a similar work, by numerical and experimental study Camilleri et al. [6] predicted out of plane distortions in double-sided butt and fillet welds attachment. A second-order quadratic mathematical model was also adapted by Gunuraj and Murugan [7]. It was concluded that for the different regions of heat affected zone, wire feed rate and welding speed had a strong effect on angular distortion. Tian et al. [8] utilized a finite element based neural network model to determine deformation induced by GTAW. The findings indicate that the distortion increases at a maximum point with the threshold of heat input and then decreases with a further increase in heat input. Dogan et al. [9] also did experiments on angular distortion and developed a mathematical model using statistical methods. It was observed that welding voltage had a strong effect on the distortion of the welded material.

Thin sheets, materials whose coefficient of thermal expansion is very large are more susceptible to distortion [10,11]. The amount of heat input generated at the weld joint significantly affects the distortion of the weldments. However, when the welding parameters are kept constant properties of the material play an important role [10]. The clamps and fixture used during welding have a definite effect on the distortion, and thus an appropriate selection of the clamping conditions is an utmost necessity [12,13]. Initial gap and misalignment have a significant influence on welding distortion as discussed by Deng et al. [14]. The deformation of the weldments has a detrimental effect on the structural integrity, quality, and performance of a weldment, thereby increasing the time consumed and cost involved.

Received: 22 Sep., 2022. Accepted: 05 Apr., 2023.

E-mail: mayuri.prod@nitjsr.ac.in (MB)



This is an Open Access article distributed under the terms of the [Creative Commons Attribution license](https://creativecommons.org/licenses/by-nc/4.0/), which permits unrestricted use, distribution, and reproduction in any medium, provided the original work is properly cited.

Li et al. [15] worked on a thin plate butt-weld and concluded that distortion of plate through experimental and numerical simulation deformation mode such as concave-convex shape occurred due to high transverse tensile stress on the upper surface at fusion zone. Huang et al. [16] also observed that distortion is affected due to the clamping condition at the welding track. Wang et al. [17] studied on welding of thin sheets and found that angular distortion is obtained due to temperature gradient through plate thickness and bending moment caused by residual plastic strain obtain in the thickness direction. Sun and Yu [18] conducted an experiment of multilayer butt-weld on 22SiMn2TiB steel a metallurgical phase transformation is taken and martensite structures are formed at the time of cooling at the welding zone and also residual stress and distortion are predicted. Akhyar et al. [19] also studied on A36 steel and concluded that distortion profiles are formed due to the cooling rate at the fusion zone and torsion was created and they also found that cooling rate also effect the hardness value at HAZ based on grain size. The importance of properties on the weld joint quality was investigated by Desai and Bag [20] both experimentally and numerically. It they concluded that mechanical and thermal properties (conductivity) greatly affect the weld joint quality. With an increase in thermal conductivity the weld bead width decreases and HAZ increases

Accurate quantitative estimation of welding deformation as well as mechanical properties are the main highlights of the paper. The current investigations include plasma arc micro welding carried out on 0.5 mm thick sheet of SS304 alloy to characterize the effect of welding parameters i.e., rate of flow of main gas for welding and welding current. The proper ranges of welding current at constant welding speed for two different rates of flow of main gas for welding are evaluated to obtain better quality of weld.

2. Experimental Procedure

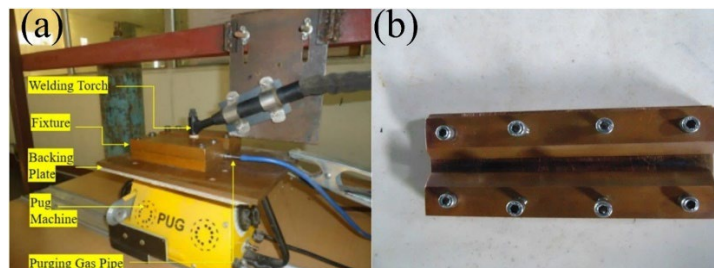


Figure 1. (a) Experimental setup; (b) Fixture used.

Table 1. Micro-Plasma Arc Welding (MPAW) process parameters used in present investigation.

Welding Parameters	Values
Welding Current	9 A,10 A,11 A
Rate of flow of main gas for welding	3.5 Lpm, 6 Lpm
Welding speed	4.2 mm/s
Copper Nozzle diameter	1.2 mm
Electrode diameter	1.2 mm
Nozzle to plate distance	2 mm
Shielding gas flow rate	0.4 Lpm
Pre Flow	4 s
Post Flow	4 s
Torch Position	Vertical

The experimental setup used in the current research for experimental purpose is shown in the Figure 1a. Industrial pure argon gas (99.9%) is used for shielding as well as plasma gas. The fixed MPAW process parameters determined by experimental trial and errors and their values are presented in Table 1. The butt welding for different current and two different plasma gas flow rate at the same speed are carried out on 0.5 mm thick SS304 sheets to evaluate the interactive influence of process parameters and to obtain practical conditions for welding. The minimum current required to generate a stable arc in the current setup is 7 A However, only heating of the plate was seen below 9A. So current values of 9A, 10 A and 11A for the present investigation. Similarly minimum gas flow rate for the arc to take place is 2 LPM. So, 3.5 LPM and 6 LPM is chosen to mark the effect of gas flow rate. The fixture used for holding the samples is made of copper as it is a good conductor of heat. The fixture design is shown in Figure 1b. The sheets are clamped properly throughout their length. Only a small opening near the weldline is open to the air for passing the torch. The wt. % of the elemental distribution of the alloy is provided in the Table 2 and tested using X-ray photoelectron spectroscopy. The weld beads formed at different current and gas flow rates ((a)10 A and 3.5 Lpm;

(b) 10A, 6 Lpm; (c) 9A Lpm; (d) 11A, 6Lpm)) are presented in Figure 2. The beads width is found to increase with current and gas flow rate due to higher heat input. Figure 2e-2f reveal the heating and burnt through of the material.

Table 2. Chemical composition of Stainless Steel 304L (weight %).

Elements	C	Si	Mn	Cr	Ni	Mo	S	P	Fe
Contents	0.023	0.36	1.54	19.01	8.27	0.305	0.01	0.001	Bal.

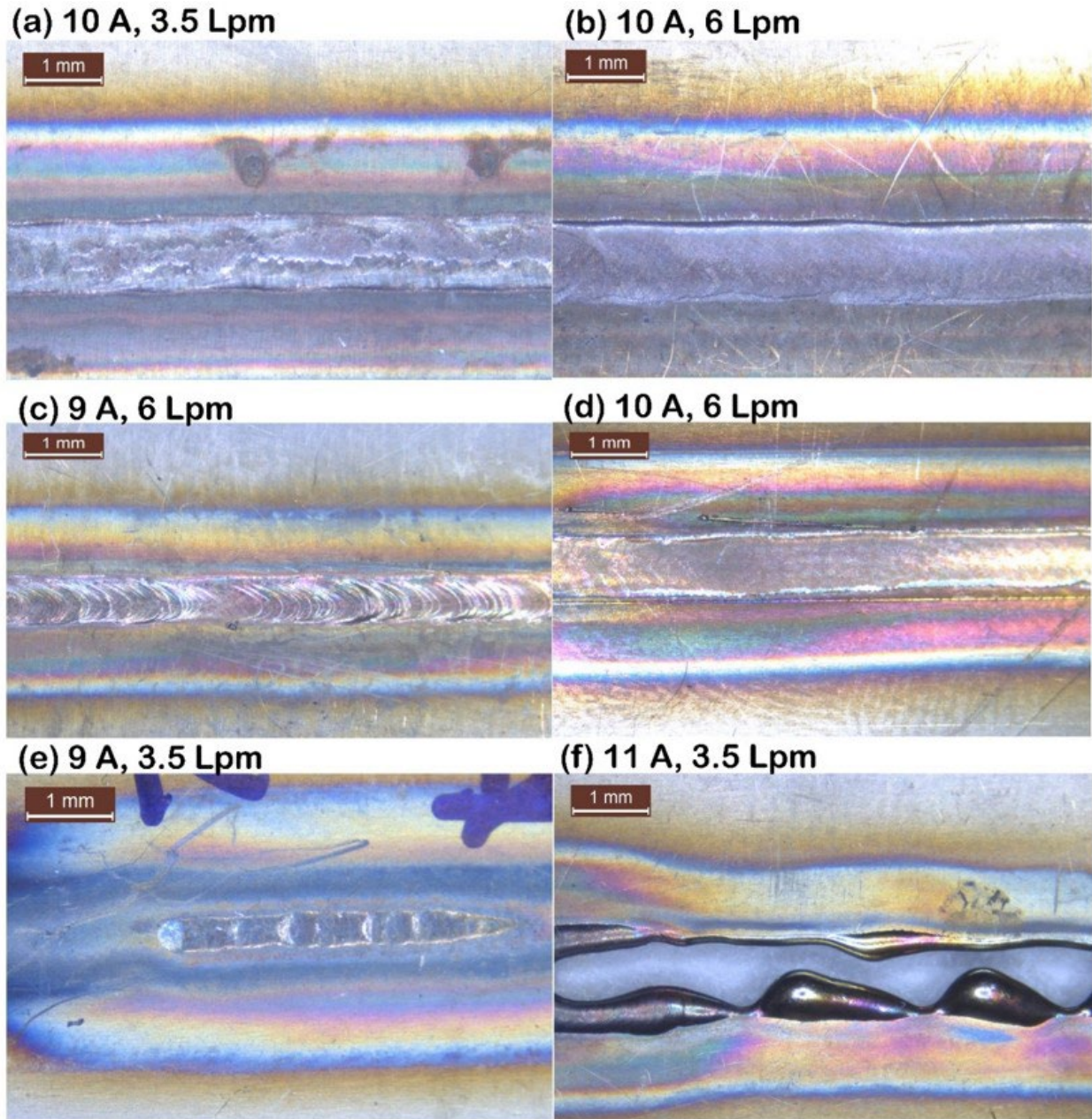


Figure 2. Weld Bead at current and gas flow rate of: (a) 10 A and 3.5 Lpm; (b) 10A, 6 Lpm; (c) 9A Lpm; (d) 11A, 6Lpm; (e) Heating at low heat input; (f) Burnt through due to high heat input.

3. Residual Distortion Measurement

The basic need to study the angular distortion in welded plate is to investigate the residual stresses induced during welding which is detrimental to the integrity and the service behavior of the welded parts. In welding, highly localized heating is done on the plate or on the joint part which leads to non-uniform stress in the component because of expansion and contraction of the heated region. At first compressive stresses induced in the cold metal at the time when weld pool is formed due to thermal expansion of the heat affected zone. If all the stresses generated from thermal expansion or contraction exceeds the yield

strength of the particular metal distortion occurs due to the plastic deformation of the metal. The distortion of the sheets as seen in Figure 3a were measured by coordinate measuring method. The method of measurement is demonstrated in Figure 3b. The longitudinal and transverse shrinkage are measured to compare the effect of current and gas flow rate.

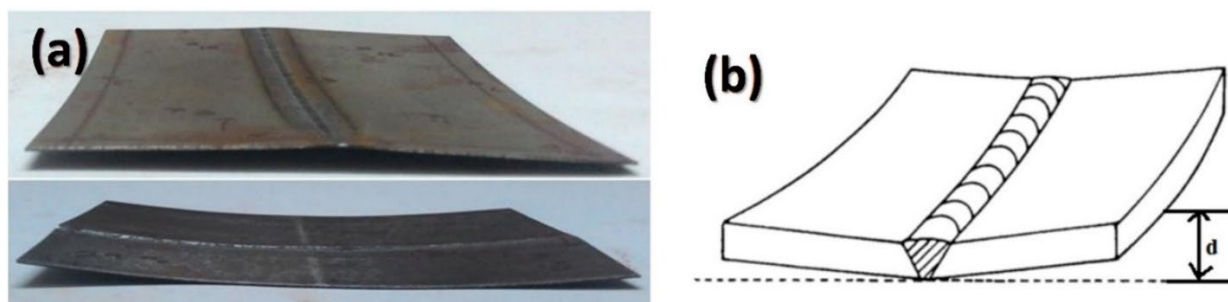


Figure 3. (a) Distortion pattern of the welded sheets; (b) Schematic image of measuring the deflection in the butt-welded joint.

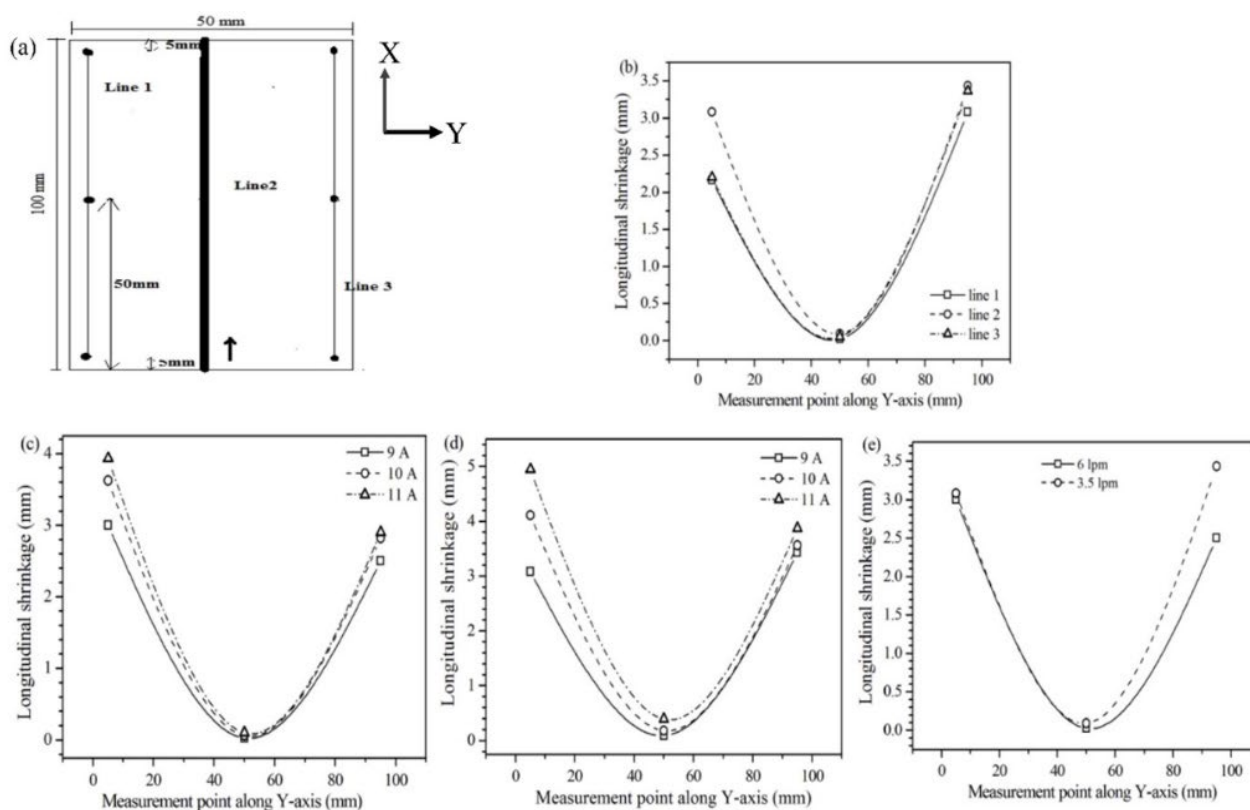


Figure 4. Longitudinal shrinkage: (a) measurement points; (b) for 9A current and 6 Lpm gas flow rate; (c) along the weld line for different currents at 3.5 Lpm gas flow rate; (d) along the weld line for different currents at 6Lpm gas flow rate; and (e) along the weld line for different plasma gas flow rate at 9A.

Figure 4 shows the longitudinal shrinkage of the plate after welding. From the Figure 4b it is seen that longitudinal distortion is more along the weld line although the pattern is the same for all the three measurement points. Figure 4c-4d show the longitudinal shrinkage along the weld line for different currents for similar gas flow rates. The longitudinal shrinkage increases with increase in current as the heat input increases. Figure 4e shows the longitudinal shrinkage along the weld line for different plasma gas flow rates at a current of 9A and all other parameters kept constant. It is found to be greater for higher gas flow rate. An increase in longitudinal shrinkage with current as well as gas flow rate is mainly due to higher heat available at a given area. This increases the temperature of a given region leading to more distortion [4,8]. Figure 5 shows the transverse shrinkage of the plate after welding. The value is found to be highest at the weld line for all the cases. Figure 5b shows that the transverse shrinkage is the highest at the edges of the plate. Similar to the longitudinal shrinkage transverse shrinkage also increases with the increase in current and plasma gas flow rate. Figure 5c-5d shows transverse shrinkage at the different welding current and also shows that with an increase in the current value the shrinkage increases due to the increase in the heat input. Figure 5e shows transverse shrinkage at the different plasma gas flow rates at a constant current of 9 A.

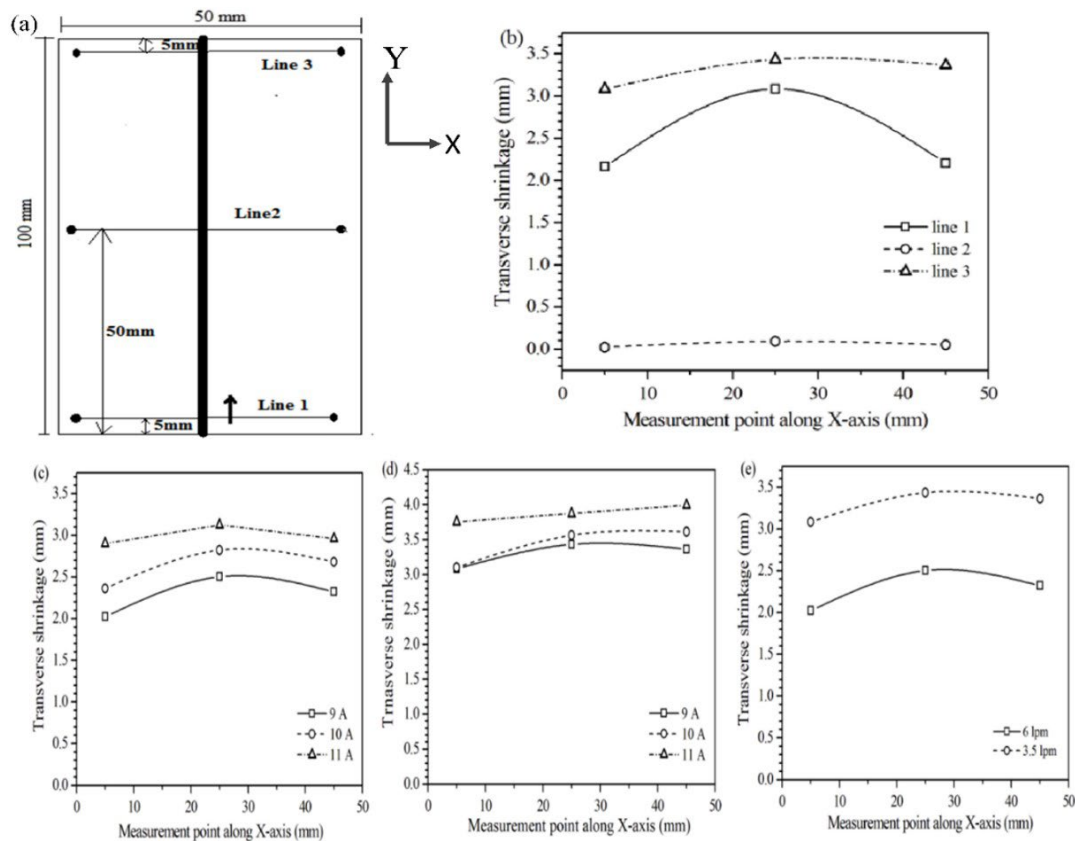


Figure 5. Transverse shrinkage: (a) measurement points; (b) for 9A current and 6 Lpm gas flow rate; (c) for different currents at 3.5 Lpm gas flow rate; (d) for different currents at 6 Lpm gas flow rate; and (e) different plasma gas flow rates.

4. Transverse Tensile Test

After the experiments, specimens were prepared for different testing for evaluating the performance of the welding procedure. For tensile testing specimens were cut by WEDM machine as per ASTM D-1708 specification. Figure 6 shows figure of samples prepared for tensile testing. This is the basic test to check the design strength requirements of a welded component. The specimens are cut at an orientation which is at right angles to the axis of the weld. The test reflects the tensile strength of the material, the pattern of failure, and the location of the fracture. Three sets of samples were prepared for each set of process parameters for tensile testing. A constant strain rate of 0.2mm/min was maintained throughout the testing. Tensile tests were carried out in 5 KN computer-controlled micro test machine (model no-MT 10081), so that specimen undergoes deformation. From Figure 6b it is seen that the fractures took place in a cup and cone style and in the HAZ zone.

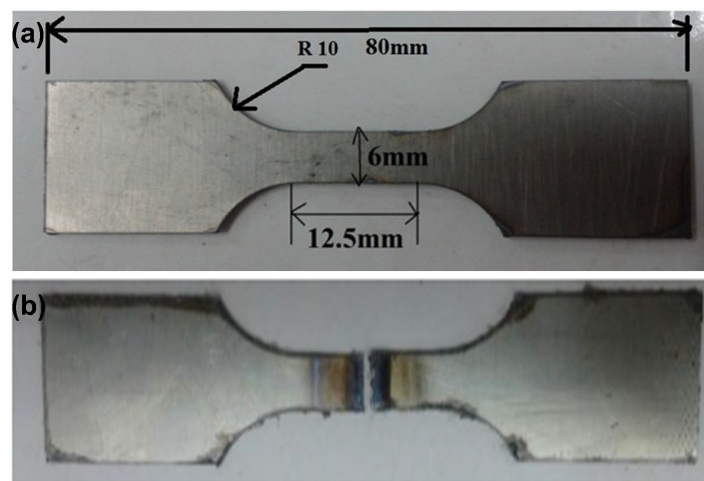


Figure 6. Dimension of specimen for tensile test.

The ultimate tensile strength of the joints for three different currents at 3.5 Lpm and 6 Lpm are plotted in Figure 7a and Figure 7b respectively. It is found that the tensile strength at all the parameters is comparable to that of the base material in the investigated range. At a lower value of current the heat generated was not sufficient to weld the samples and create a defect weld. At higher values of current, the excess current amplitude is leading to the spatter of weld pool and again reduces the strength of the weld. The optimum value of current is found to be 10 A. The stress- strain graph is plotted as shown in Figure 7c at optimum current (10A). It is found that the ultimate tensile strength of SS304 welded at 6 Lpm with all other parameters remaining constant is slightly more than that of 3 Lpm.

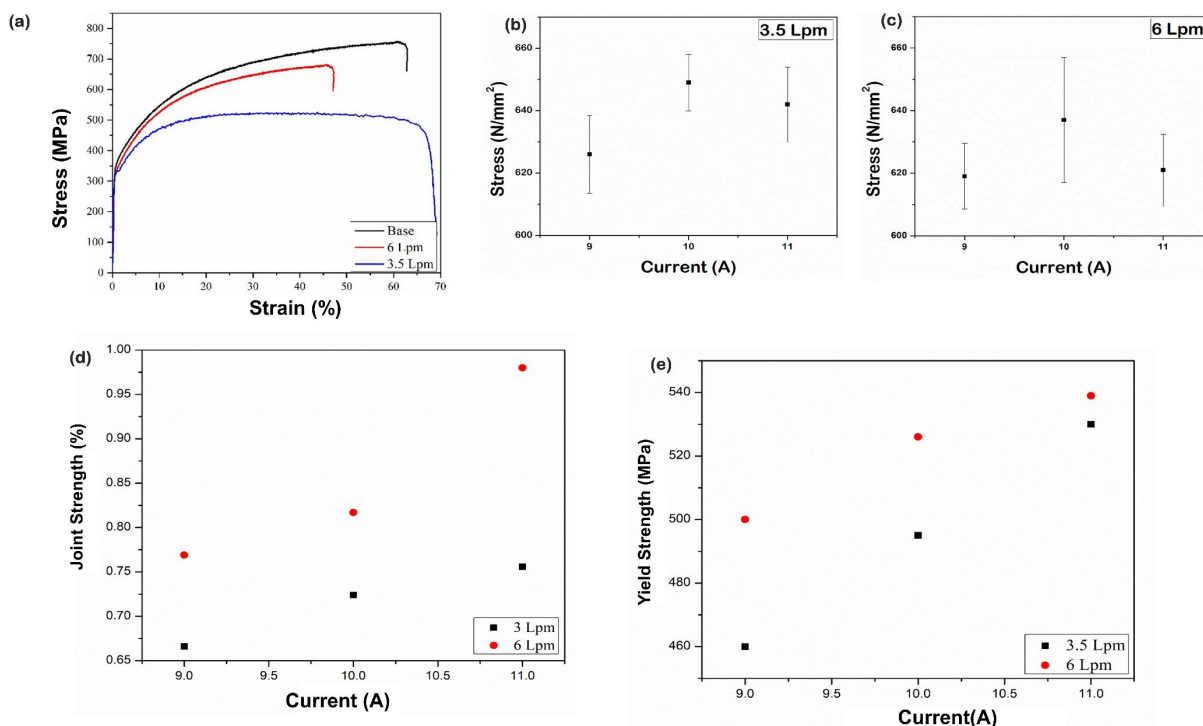


Figure 7. (a) Stress Vs strain curve at different gas flow rate at constant current of 9A; Current Vs Ultimate tensile stress at (b) 3.5 Lpm; (c) 6 Lpm; (d) Yield strength; (e) Joint strength.

5. Fractography

The SEM fractography of a welded joint are shown in Figure 8a-8b, exhibiting numerous dimples on the fractured surfaces reflecting that the mode of failure for the tensile test is ductile thus and the specimens are subjected to large plastic deformation prior to failure. In Figure 8a more number of shallow dimples are observed which indicate moderate ductility suggesting the formation of lamellar structure (20). However, deeper dimples are observed in Figure 8b suggesting martensitic structure formation having good ductility (20) due to increased cooling rate.

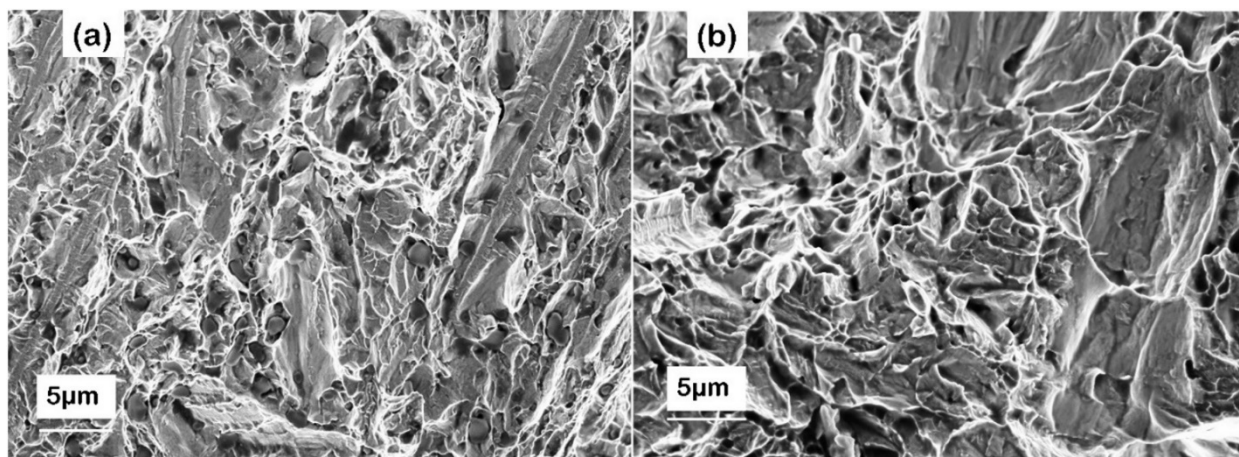


Figure 8. Fractography of samples at 10 A and gas flow rate of (a) 3.5 Lpm; (b) 6 Lpm.

6. Hardness

After Micro plasma arc welding at different process parameter, specimens at each parameter are prepared and average hardness is measured at five different points on specimen. The distance between the points is 1 mm so as to record the hardness values at each zone, Vickers hardness testing is carried out with 300 kgf load for getting the indentation. The location of 5 points is marked in Figure 9a. The hardness value is found to increase at weld nugget zone (258 HV) at 6 Lpm. The hardness profiles of sample at 10 A and gas flow rate of 3.5 Lpm and 6 Lpm as compared to the base metal are depicted in Figure 9b. Point 3 is falling in fusion zone (FZ) which is showing maximum hardness at both the gas flow rate. In the weld zone due to the higher cooling rate chances of forming martensitic structure is highest than the HAZ (13).

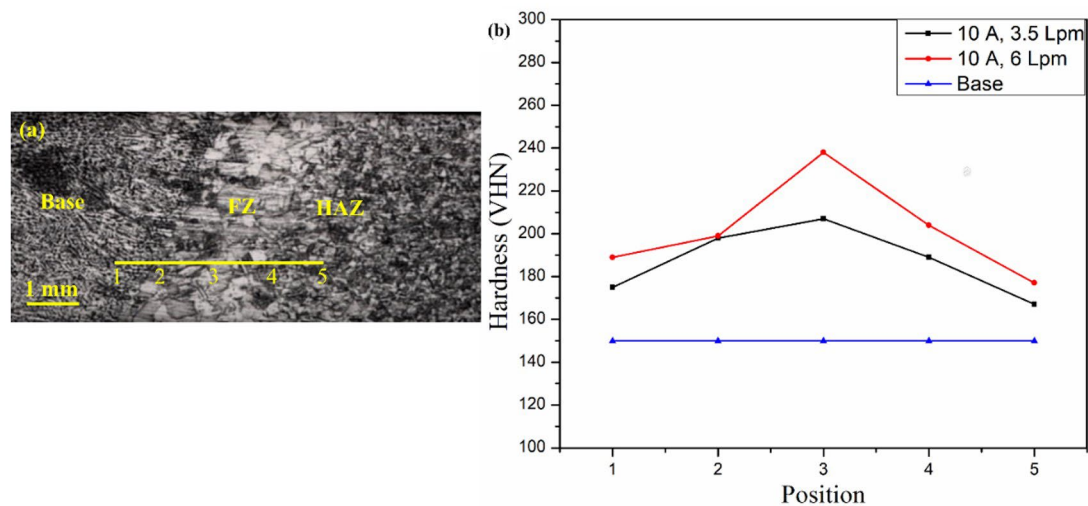


Figure 9. (a) Hardness profiles of sample at 10 A and gas flow rate of 3.5 Lpm and 6 Lpm, and (b) Hardness plot at different position and gas flow rate.

7. Conclusions

Experiments have been performed on SS304 alloy to weld at three different currents for two gas flow rate and constant velocity. Distortion analysis is done with the help of coordinate measuring machine. The distortion is mainly due to the sudden contraction and expansion of the HAZ (heat affected zone). Mechanical properties are evaluated by hardness test, tensile test and fractography. Thus, this paper suggests a suitable method for joining thin sheets with reduced distortion. This may serve as a basis for microwelding of other materials and thickness. This study also highlighted that an optimum heat input is utmost necessities in microwelding. From present investigation the following conclusions are drawn.

- It is found that the longitudinal shrinkage is higher compare to the transverse shrinkage in the welded sheets. Bending is the highest at the edge of the plate in the weld line compared to the other portion of the plate. An interesting fact is that the transverse shrinkage is lower on the side from where welding is started, compared to the other extreme edge.
- Distortion analysis is done on different parameters and it is found that plasma flow rate and welding current have positive effect to the distortion extent that is distortion increases with increasing plasma flow rate as well as welding current. This is because with increase in gas flow rate and current more heat is applied at a given area leading to greater distortion.
- With the increasing welding current, it can be seen that weld bead width also increases. As the current increases so the heat input also increases which results in larger weld bead width (Figure 2). It is found that weld dimension is more at higher rate of flow of main gas for welding. Heat input is also an important parameter for predicting welding distortions.
- Hardness and tensile properties were found comparable to the base material in the given range of process parameters.

Authors' contributions

KA: writing, data analysis, data curation. MB: writing and editing, conceptualization, supervision.

Acknowledgements

The authors wish to acknowledge National Institute of technology Jamshedpur for conducting this research work. The authors would also like to express their gratitude to the ASR metallurgy and auto cluster Jamshedpur for UTM, Hardness and CMM (Distortion).

References

- [1] Choobi MS, Haghpanahi M, Sedighi M. Prediction of welding-induced angular distortions in thin butt-welded plates using artificial neural networks. *Computational Materials Science*. 2012;62:152-159. <http://dx.doi.org/10.1016/j.commatsci.2012.05.032>.
- [2] Murugan VV, Gunaraj V. Effects of process parameters on angular distortion of gas metal arc welded structural steel plates. *Welding Journal*. 2005;84(11):165S-171S.
- [3] Deng D. FEM prediction of welding residual stress and distortion in carbon steel considering phase transformation effects. *Materials & Design*. 2009;30(2):359-366. <http://dx.doi.org/10.1016/j.matdes.2008.04.052>.
- [4] Long H, Gery D, Carlier A, Maropoulos PG. Prediction of welding distortion in butt joint of thin plates. *Materials & Design*. 2009;30(10):4126-4135. <http://dx.doi.org/10.1016/j.matdes.2009.05.004>.
- [5] Deng D, Murakawa H. Prediction of welding residual stress in multi-pass butt-welded modified 9Cr–1Mo steel pipe considering phase transformation effects. *Computational Materials Science*. 2006;37(3):209-219. <http://dx.doi.org/10.1016/j.commatsci.2005.06.010>.
- [6] Camilleri D, Comlekci T, Gray TGF. Thermal distortion of stiffened plate due to fillet welds computational and experimental investigation. *Journal of Thermal Stresses*. 2006;29(2):111-137. <http://dx.doi.org/10.1080/01495730500257441>.
- [7] Gunaraj V, Murugan N. Prediction of heat-affected zone characteristics in submerged arc welding of structural steel pipes. *Welding Journal*. 2002;81(3):94S-98S.
- [8] Tian L, Luo Y, Wang Y, Wu X. Prediction of transverse and angular distortions of gas tungsten arc bead-on-plate welding using artificial neural network. *Materials & Design*. 2014;54:458-472. <http://dx.doi.org/10.1016/j.matdes.2013.08.082>.
- [9] Dogan E, Ay M, Kurtulmus M, Yukler AI, Etyemez A. Effects of welding parameters on the angular distortion of welded steel plates. *Open Chemistry*. 2022;20(1):417-423. <http://dx.doi.org/10.1515/chem-2022-0152>.
- [10] Wang J, Feng JC, Wang YX. Microstructure of Al-Mg dissimilar weld made by cold metal transfer MIG welding. *Materials Science and Technology*. 2008;24(7):827-831. <http://dx.doi.org/10.1179/174328408X278411>.
- [11] McDill JMJ, Oddy AS, Goldak JA, Bennison S. Finite element analysis of weld distortion in carbon and stainless steels. *Journal of Strain Analysis*. 1990;25(1):51-53. <http://dx.doi.org/10.1243/03093247V25I051>.
- [12] Schenk T, Richardson IM, Kraska M, Ohnimus S. A study on the influence of clamping on welding distortion. *Computational Materials Science*. 2009;45(4):999-1005. <http://dx.doi.org/10.1016/j.commatsci.2009.01.004>.
- [13] Arunkumar M, Dhinakaran V, Sivashanmugam N, Petley V. Effect of plasma arc welding on residual stress and distortion of thin titanium sheet. *Materials Research*. 2019;22(6):e20190366. <http://dx.doi.org/10.1590/1980-5373-mr-2019-0366>.
- [14] Deng D, Murakawa H, Liang W. Numerical simulation of welding distortion in large structures. *Computer Methods in Applied Mechanics and Engineering*. 2007;196(45-48):4613-4627. <http://dx.doi.org/10.1016/j.cma.2007.05.023>.
- [15] Li X, Hu L, Deng D. Influence of contact behavior on welding distortion and residual stress in a thin-plate butt-welded joint performed by partial-length welding. *Thin-walled Structures*. 2022;176:109302. <http://dx.doi.org/10.1016/j.tws.2022.109302>.
- [16] Huang H, Chen J, Feng Z, Wang HP, Cai W, Carlson BE. Large-scale welding process simulation by GPU parallelized computing. *Welding Journal*. 2021;100(11):359S-370S. <http://dx.doi.org/10.29391/2022.101.032>.
- [17] Wang J, Zhou X, Yi B. Buckling distortion investigation during thin plates butt welding with considering clamping influence. *CIRP Journal of Manufacturing Science and Technology*. 2022;37:278-290. <http://dx.doi.org/10.1016/j.cirpj.2022.02.008>.
- [18] Sun Z, Yu X. Prediction of welding residual stress and distortion in multi-layer butt-welded 22SiMn2TiB steel with LTT filling metal. *Journal of Materials Research and Technology*. 2022;18:3564-3580. <http://dx.doi.org/10.1016/j.jmrt.2022.04.031>.
- [19] Akhyar, Tamlicha A, Farhan A, Azwinur, Syukran, Fadhilah TA, et al. Evaluation of welding distortion and hardness in the A36 steel plate joints using different cooling media. *Sustainability*. 2022;14(3):1405. <http://dx.doi.org/10.3390/su14031405>.
- [20] Desai RS, Bag S. Influence of displacement constraints in thermomechanical analysis of laser micro-spot welding process. *Journal of Manufacturing Processes*. 2014;16(2):264-275. <http://dx.doi.org/10.1016/j.jmapro.2013.10.002>.